Antibody-Induced Conformational Changes in the *Torpedo* Nicotinic Acetylcholine Receptor: A Fluorescence Study†

C. Fernando Valenzuela,‡,§ Alan J. Dowding,‖,⊥ Hugo R. Arias,‡,# and David A. Johnson*,‡

Division of Biomedical Sciences and Department of Neuroscience, University of California, Riverside, California 92521-0121, and University of California, San Francisco, California 94143-0444

Received December 27, 1993; Revised Manuscript Received March 29, 1994®

ABSTRACT: Quantitative fluorescence spectroscopy was used to develop a structural picture of the effects of two monoclonal antibodies (mAbs) on the conformation of the *Torpedo* nicotinic acetylcholine receptor (nAChR). The two mAbs (*A6* and *B1*) examined selectively blocked ligand binding to either the high-affinity (*A*) or the low-affinity (*B*) binding sites for agonists/competitive antagonists. The distances between dansyl-C_6-choline bound to the unblocked agonist/competitive antagonist binding site and one of two lipophilic probes (C_{12}-eosin or C_{18}-rhodamine) partitioned into the lipid membrane were estimated by using fluorescence resonance energy transfer. Control experiments demonstrated that both mAbs decreased the affinity and fluorescence lifetime of receptor-bound dansyl-C_6-choline. The binding of the *B1* mAb to the *B* site did not significantly change the calculated distance between the unblocked *A* binding site and the membrane surface. However, the binding of the *A6* mAb to the *A* site induced the *B* site to move into close proximity to the lipid membrane. This conformational change was confirmed by a 45-fold increase in the paramagnetic quenching of the *B*-site-bound dansyl-C_6-choline fluorescence by lipid-intercalated 5-doxylstearate. The results indicate that these mAbs not only selectively block ligand binding to either the *A* or the *B* acetylcholine sites but also, in the case of the *A6* mAb, induce global conformational changes of the receptor, which appear to involve a movement of the *B* binding site into close proximity of the lipid membrane. Because mAbs can induce substantial changes in the position of functional domains of the nAChR, mAbs appear to have the potential of dramatically altering epitope locations, and consequently, conflicting results can potentially arise when mAbs are used to delineate structural details of the nAChR.

The muscle-type nicotinic acetylcholine receptor (nAChR)[1] is a pentameric ligand-gated ion channel that is formed by four subunits (α, β, γ, and δ) in a stoichiometric ratio of 2:1:1:1 [for reviews see Galzi *et al.* (1991) and Karlin (1991)]. Cholinergic agonists (e.g., acetylcholine and carbamylcholine) and competitive antagonists (e.g., α-bungarotoxin and *d*-tubocurarine) bind to two sites located in the extracellular domain of the receptor, 30–40 Å above the lipid membrane surface (Unwin, 1993; Valenzuela *et al.*, 1994). These two agonist/competitive antagonist (ACh) binding sites are nonequivalent, evidenced by the differential affinity of [^{3}H]-*d*-tubocurarine toward these sites (Neubig & Cohen, 1979). Further support for the nonequivalence of the ACh binding sites stems from the development of monoclonal antibodies (mAbs) that selectively recognize and block ligand binding to either the high-affinity (the *A* site) or the low-affinity (the *B* site) ACh binding sites (Dowding & Hall, 1987).

The interaction of specific antibodies with the nAChR has been the focus of intense research because of their involvement in the pathogenesis of the neuromuscular disease myasthenia gravis [reviewed in Tzartos *et al.* (1991)]. Monoclonal antibodies to the nAChR have been instrumental in the elucidation of (*i*) the synthesis, assembly, and transmembrane topology of nAChR subunits (Karlin *et al.*, 1986; Lindstrom, 1986; Lei *et al.*, 1993); (*ii*) the localization, structure, and pharmacological properties of the ACh binding sites (Conti-Tronconi *et al.*, 1990; Dowding & Hall, 1987; Klymkowsky *et al.*, 1979); and (*iii*) the characterization of neuronal nAChRs (Arnand *et al.*, 1991; Role, 1992). Although mAbs have played a crucial role in the development of our knowledge of the nAChR, little is known about their effects on both the function and the conformation of the nAChR [for a review see Maelicke *et al.* (1988)].

Pharmacological and biochemical evidence suggests that mAbs can induce significant conformational changes in the nAChR. Fels *et al.* (1986) demonstrated that an anti-α subunit mAb allosterically blocks ligand binding to the ACh binding sites. Moreover, Chinchetru *et al.* (1989) have identified a mAb that noncompetitively blocks agonist-induced fluxes into nAChR-rich vesicles without interacting with either

† This work was supported by Grant 91-140 to D.A.J. from the American Heart Association (California Affiliate) and a postdoctoral fellowship from the Argentinian Consejo Nacional de Investigaciones Científicas y Técnicas (CONICET) to H.R.A.

* Address correspondence to this author at Division of Biomedical Sciences, University of California, Riverside, CA 92521-0121 [telephone (909) 787-3831; fax (909) 787-5504].

‡ University of California, Riverside.

§ Present address: Department of Pharmacology, University of Colorado Health Sciences Center, Denver, CO 80262.

‖ University of California, San Francisco.

⊥ Present address: MRC Muscle and Cell Motility Unit, King's College London, 26-29 Drury Lane, London WC2B 5RL, U.K.

Present address: Instituto de Investigaciones Bioquímicas de Bahía Blanca (INIBIBB), Camino La Carrindanga km 7, C.C. 857, Bahía Blanca 8000, Argentina.

® Abstract published in *Advance ACS Abstracts,* May 15, 1994.

[1] Abbreviations and trivial names: ACh binding sites, sites of binding of agonists and competitive antagonists; *A* binding site, high-affinity ACh binding site at the α–γ subunit interface; *B* binding site, low-affinity ACh binding site at the α–δ subunit interface; buffer I, 100 mM NaCl, 10 mM sodium phosphate, pH 7.4; C_{12}-eosin; 5-(dodecanoylamino)eosin; C_{12}-fluorescein, 5(dodecanoylamino)fluorescein; C_{18}-rhodamine, octadecylrhodamine B; cobra α-toxin, *Naja naja siamensis* 3 α-toxin; dansyl-C_6-choline, 6-[5-(dimethylamino)naphthalene-1-sulfonamido]hexanoic acid β-(*N*-trimethylammonium)ethyl ester; FRET, fluorescence resonance energy transfer; mAbs, monoclonal antibodies; nAChR, nicotinic acetylcholine receptor; PCP, phencyclidine; SCID, severe combined immunodeficiency.

0006-2960/94/0433-6586$04.50/0

the ACh or the traditional noncompetitive inhibitor binding sites. The physical basis of these or, in fact, any mAb-induced conformational changes has yet to be elucidated.

In this paper, the effects of two ACh binding site-specific mAbs on the conformation of the nAChR were examined. The two mAbs examined were the *A6* and the *B1* developed by Dowding and Hall (1987), which recognize and block ligand binding to the *A* and the *B* ACh binding sites, respectively. These mAbs were used to direct the binding of a fluorescence agonist, dansyl-C_6-choline, to the unblocked ACh binding site. Fluorescence resonance energy transfer (FRET) and paramagnetic quenching techniques were then used to assess the mAb-induced changes in the distance between receptor-bound dansyl-C_6-choline and the lipid–membrane surface. The results indicate a differential ability of the two mAbs examined to alter the proximity of the ACh binding sites to the lipid membrane.

EXPERIMENTAL PROCEDURES

Materials. 5-(*N*-Dodecanoyl)aminofluorescein (C_{12}-fluorescein), 5-(*N*-dodecanoyl)aminoeosin (C_{12}-eosin), and octadecylrhodamine B (C_{18}-rhodamine) were purchased from Molecular Probes (Eugene, OR). *Torpedo californica* electric rays were obtained from Marinus Inc. (Long Beach, CA). Phencyclidine (PCP), 6-doxylstearate, carbamylcholine, and suberyldicholine were from Sigma (St. Louis, MO). *Naja naja siamensis* 3 α-toxin (cobra α-toxin) was isolated following the method of Karlsson *et al.* (1971) from *N. naja siamensis* venom purchased from the Miami Serpentarium (Salt Lake City, UT). Dansyltrimethylamine perchlorate was acquired from Pierce Chemical Co. (Rockford, IL). 3-[^{125}I](Iodotyrosyl^{54})-α-bungarotoxin ([^{125}I]iodo-α-bungarotoxin) was obtained from Amersham (Arlington Heights, IL). Hybridomas producing the *A1* and *B6* type mAbs were generously provided by Dr. Zach Hall (University of California, San Francisco). RPMI 1640 tissue culture media, penicillin–streptomycin, and L-glutamate were from Fisher (Tustin, CA). Severe combined immunodeficient (SCID) mice were generously provided by Dr. Ken Dorshkind (University of California, Riverside). 6-[(5-Dimethylamino)naphthalene-1-sulfonamido]hexanoic acid β-(*N*-trimethylammonium)ethyl ester (dansyl-C_6-choline) was synthesized as described elsewhere (Valenzuela *et al.*, 1994).

Receptor Isolation. Base-treated nAChR-associated membranes were isolated from the *T. californica* electric organ by established procedures (Johnson & Yguerabide, 1985). The receptor-specific activities were determined by the decrease in dansyltrimethylamine (6.6 μM) fluorescence produced by the titration of suberyldicholine into receptor suspensions (0.3 mg of protein/mL plus 100 μM PCP), following a modification of the method of Neubig and Cohen (1979). The receptor-specific activities ranged between 1.0 and 2.2 nmol of suberyldicholine binding sites/mg of protein.

mAb Production. Hybridomas of the *A6* and *B1* mAbs were grown in RPMI 1640 media, supplemented with 10% fetal bovine serum and 1% penicillin–streptomycin. Hybridomas were grown as ascites in severe combined immunodeficient mice to produce high levels as described by Ware *et al.* (1985).

Quantification of mAb Binding. The mAb concentrations were assessed by determining the amount mAb that would just maximally inhibit [^{125}I]iodo-α-bungarotoxin binding to a known amount of nAChR. Briefly, nAChR-associated membranes (20 nM in suberyldichloride binding sites) were resuspended in 0.15 mL of 100 mM NaCl and 10 mM $NaPO_4$, pH 7.4 (buffer I), and incubated with increasing amounts of the *A6* or *B1* mAbs or an excess amount of native cobra α-toxin (8 μM) for 90 min at 37 °C. At the end of the incubation period, the reaction tubes were centrifuged at 110000*g* for 10 min in a Beckman Airfuge, and the radioactivity in the pellets was measured. The mAb concentrations were obtained from a plot of the specific (cobra α-toxin subtracted) counts from the pellets vs the volume of mAb sample added; the point in the curve where the inhibition of [^{125}I]iodo-α-bungarotoxin binding first plateaued defined the amount of added mAb that equaled the amount of receptor present (10 nM in functional units). The total mAb concentrations in the various ascites fluids ranged between 5 and 18 μM.

Fluorescence Measurements. Steady-state fluorescence measurements were made with a Perkin-Elmer-Cetus MPF 66 spectrofluorometer. Fluorescence lifetimes were determined by the time-correlated single photon counting technique using an EEY scientific nanosecond fluorescence spectrofluorometer (La Jolla, CA), equipped with a high-pressure hydrogen arc lamp. For receptor-bound dansyl-C_6-choline, excitation and emission wavelengths were selected with a Corning 7-54 cutoff filter and an Oriel 540-nm narrow-band interference filter, respectively. A Polaroid HNPB dichroic film polarizer (Norwood, MA), rotated 55° relative to the vertical, was placed in the emission path. Fluorescence decays were analyzed with GLOBALS UNLIMITED computer program (version 1.01; Laboratory of Fluorescence Dynamics, Urbana–Champaign, IL).

Effects of mAbs on Dansyl-C_6-choline Binding. The dissociation constant (K_D) for dansyl-C_6-choline binding to the receptor was determined by the forward titration of dansyl-C_6-choline into nAChR membrane suspensions (50 nM in suberyldicholine binding sites) in buffer I plus PCP (40 μM) that were or were not previously incubated with the *A6* or *B1* mAbs (50 nM) for 90 min at 37 °C. The mAbs were incubated with the nAChR in plastic tubes to minimize their adsorption into the quartz cuvettes. A sample that was preincubated for 30 min with cobra α-toxin (8 μM) was used to determine the fluoresence from nonspecifically bound dansyl-C_6-choline. Estimates of the K_D were obtained by fitting the cobra α-toxin-sensitive dansyl-C_6-choline fluorescence vs total dansyl-C_6-choline concentration data to a four-parameter logistic (sigmoid) equation with the GraphPad computer program (GraphPad Software, San Diego, CA).

Effect of the mAbs on the Quantum Yield of nAChR-Bound Dansyl-C_6-choline. The quantum yield of nAChR-bound dansyl-C_6-choline (Q_B) was determined by using

$$Q_B = Q_F[\langle\tau\rangle_{Bound}/\langle\tau\rangle_{Free}] \quad (1)$$

where Q_F is the quantum yield of free dansyl-C_6-choline and $\langle\tau\rangle_{Bound}$ and $\langle\tau\rangle_{Free}$ are the geometrically averaged lifetimes of bound and free dansyl-C_6-choline, respectively. Equation 1 assumes that the quantum yield is proportional to the fluorescence lifetime (Berlman, 1971). The quantum yield of free dansyl-C_6-choline was determined by the ratio method of Chen (1965), with fluorescein (Q = 0.85) in 0.1 N NaOH as a standard.

FRET Model. To calculate the transverse distance between the receptor-bound donors and acceptors randomly positioned at the membrane surface, we used the Off-Axis FRET model (Yguerabide, 1994) that assumes that the donors are attached at a distance δ from the major axis of symmetry of cylindrical proteins imbedded into a planar-lipid membrane. The symmetry axis of these proteins is perpendicular to the membrane surface. The transverse distance from the protein-bound donors to the plane of acceptors positioned in the water–

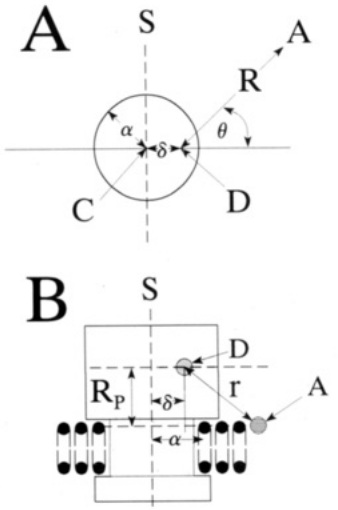

FIGURE 1: Schematic representation of the Off-Axis FRET membrane model. Panel A shows the schematic representation in the acceptor plane of the coordinate system used to describe the position of an acceptor A relative to the projection of the donor (D′) into the acceptor plane. The radius α of the circle is the distance of closest approach of acceptors to the center of the circle C. The center is the point where the transverse symmetry axis S of the cylindrically symmetric proteins intercepts the acceptor plane. δ is the distance from the symmetry axis S at the center of the circle to D′. The position of A with respect to D′ in the acceptor plane is described by the distance R and angle θ. Panel B shows a cross-sectional representation of this model. r is the distance of closest approach between the donor D and an acceptor A. Membrane-partitioned acceptors are assumed to be distributed randomly in a planar array at a distance R_P from the donors.

lipid interface is R_P. The distance of closest approach between the acceptors and the central axis of the protein in the acceptor plane is α, and α is assumed to be greater than or equal to δ. This is represented graphically in Figure 1 and is derived elsewhere (Yguerabide, 1994).

To calculate theoretical energy-transfer efficiency for this model, it is necessary to focus on the time-dependent decay of emission of the energy donor. The donor fluorescence intensity, $F(t)$, at any time t after excitation by a very short pulse of light is given by

$$F(t) = F(0)e^{-t/\tau_D}e^{-\sigma M(t)} \quad (2)$$

where τ_D is the donor fluorescent lifetime, σ is the surface density of acceptors, and $M(t)$, in turn, is defined by the following integral:

$$M(t) = 2\int_0^{\pi} S(t,\theta)d\theta \quad (3)$$

$S(t,\theta)$ is given by the integral

$$S(t,\theta) = \int_{r_c(\theta)}^{\infty}(1 - e^{(t/\tau)(R_0/r)^6})rdr \quad (4)$$

where r is the distance between donor–acceptor pairs and r_c is the distance of closest approach between donor–acceptor pairs and equals

$$r_c(\theta) = [R_p^2 + R_c^2(\theta)]^{1/2} \quad (5)$$

where

$$R_c(\theta) = -\delta\cos\theta + [\delta^2\cos^2\theta + (\alpha^2 - \delta^2)]^{1/2} \quad (6)$$

R_0 represents the Förster critical distance (in angstroms) and is defined by the expression

$$R_0 = 9.765 \times 10^3 (\kappa^2 J Q_D n^{-4})^{1/6} \quad (7)$$

The overlap integral, J, (in cm^6/mol) is calculated from the experimental spectra through the relationship

$$J = \sum I_D(\lambda)\epsilon_A(\lambda)\lambda^4\Delta\lambda / \sum I_D(\lambda)\Delta\lambda \quad (8)$$

where $\epsilon_A(\lambda)$ is the molar extinction coefficient of the energy acceptor and $I_D(\lambda)$ is the relative donor emission spectrum. Q_D denotes the donor quantum yield in the absence of acceptor, and n represents the refractive index of the medium between donor and acceptor. For proteins, the refractive index is about 1.4. λ is the wavelength in centimeters, and κ^2 is the orientation factor and accounts for the relative orientation of the donor emission and acceptor absorption transition dipoles.

The theoretical ratio of steady-state donor fluorescence in the absence over presence of acceptor (I_D/I_{DA}) is given by the integral ratio

$$\frac{I_D}{I_{DA}} = \frac{\int_0^{\infty} F_D(t)dt}{\int_0^{\infty} F_{DA}(t)dt} \quad (9)$$

where the subscripts D and DA denote the absence and presence of acceptor, respectively. The surface density of acceptor probes was determined in parallel samples by measuring FRET between membrane-partitioned C_{12}-fluorescein and C_{12}-eosin or C_{18}-rhodamine as described elsewhere (Valenzuela *et al.*, 1992).

FRET and Paramagnetic Quenching Measurements. Dansyl-C_6-choline (0.4 μM) and nAChR-associated membranes (0.4 μM in suberyldicholine binding sites) were suspended in buffer I plus PCP (100 μM) in the absence and in the presence of either the *A6* or the *B1* mAbs (0.4 μM). The mAbs and the nAChR membranes were incubated in plastic tubes at 37 °C for 90 min and then transferred to the cuvettes. Titrants were dissolved in dimethyl sulfoxide (C_{12}-eosin, 1.2 mM; C_{18}-rhodamine, 1.2 mM; and 5-doxylstearate, 12.8 mM) and added to the cuvettes with 10-μL Hamilton syringes. After each addition of titrant, the samples were incubated for 5 min before the fluorescence was measured.

Because only a fraction (f) of dansyl-C_6-choline was bound to the ACh binding sites, calculation of the specific FRET and paramagnetic quenching required separation of the receptor-bound (I_B) from the free dansyl-C_6-choline fluorescence. This was accomplished by using the expression

$$I_B = C_d[(I_{\text{minus tox}} - I_{blk}) - (1 - f)(I_{\text{plus tox}} - I_{blk})] \quad (10)$$

where $I_{\text{plus tox}}$ and $I_{\text{minus tox}}$ are the magnitudes of fluorescence of samples that did or did not contain an excess of cobra α-toxin, respectively (Valenzuela *et al.*, 1992, 1994). I_{blk} is the magnitude of the intrinsic fluorescence of the samples in the absence of dansyl-C_6-choline, and C_d is a correction factor for dilution and inner filter effects of the titrant. The correction for inner filter effects was calculated as described by Valenzuela *et al.* (1992). The fraction of nAChR-bound dansyl-C_6-choline was determined from a plot of the cobra α-toxin-sensitive dansyl-C_6-choline fluorescence vs the total titrated concentration of dansyl-C_6-choline.

For the FRET experiments, the ratio of the bound dansyl-C_6-choline fluorescence in the absence over the presence of acceptor (I_D/I_{DA}) was plotted as a function of the acceptor surface density, σ, times R_o^2 and the slope was calculated. The transverse distance, R_P, was then read off a second plot

(slope vs R_P) generated by calculating the slopes of theoretical plots of I_D/I_{DA} vs σR_0^2 (using eqs 2–9) for different values of R_P.

For the paramagnetic quenching experiments, the bound dansyl-C_6-choline or the C_{18}-rhodamine fluorescence in the absence over presence of lipophilic quencher was plotted as a function of the concentration of added quencher. The slopes of these plots defined the apparent Stern–Volmer quenching constant, K_Q, and provided a measure of the accessibility of the quencher to the fluorophore. Because of the restricted rotational freedom and relatively short fluorescence lifetimes of both fluorophores (<15 ns) when associated with the nAChR membranes, no effort was made to correct for differences in their fluorescence lifetimes (London, 1982).

Relative Sensitivity of Dansyl-C_6-choline and C_{18}-Rhodamine to Nitroxide Quenching. The relative sensitivities to paramagnetic quenching were assessed by comparison of the bimolecular quenching rate constants, k_q, of dansyl-C_6-choline and C_{18}-rhodamine in 1-butanol with Tempo as a nitroxide quencher. The k_q values were determined by measuring the fluorescence lifetimes of the two fluorophores in the absence, τ_0, and the presence, τ, of various concentrations of Tempo. The results were then analyzed with the lifetime Stern–Volmer expression

$$\tau_0/\tau = 1 + K_Q'[Q] = 1 + k_q\tau_0[Q] \qquad (11)$$

where K_Q' is the lifetime Stern–Volmer quenching constant.

The excitation wavelength for dansyl-C_6-choline was selected with a Corning 7-60 interference filter, and the emission was selected with a Corning 3-71 cutoff filter. For C_{18}-rhodamine the excitation and emission wavelengths were selected by using an Oriel 560 nm narrow-band interference filter and a Corning 3-66 cutoff filter, respectively. Stock solutions of Tempo (4.75 M) were freshly prepared in 1-butanol.

RESULTS

mAb Effects on Dansyl-C_6-choline Binding. To quantitate the FRET between receptor-bound dansyl-C_6-choline and the membrane-partitioned probes, the effect of the mAbs on the affinity of dansyl-C_6-choline toward the unblocked ACh binding sites was determined by direct fluorescence titration. The concentration dependencies of cobra α-toxin-sensitive dansyl-C_6-choline binding to the ACh binding sites with and without the mAbs are shown in Figure 2. The binding affinity of dansyl-C_6-choline toward the unblocked ACh binding sites was reduced by both the *A6* and *B1* mAbs. In the absence of mAbs, the apparent K_D of dansyl-C_6-choline toward the receptor was 20 ± 14 nM (nine determinations) (Valenzuela *et al.*, 1994), and it increased to 117 ± 14 (four determinations) and 75 ± 11 nM (four determinations) by the presence of the *A6* and the *B1* mAbs, respectively. In addition, the *A6* and *B1* mAbs decreased the apparent Hill slope from a value of 1.8 to near unity (0.96 and 0.82, respectively), a finding consistent with the mAbs blocking the normally cooperative interaction between the *A* and *B* ACh sites.

mAb Effects on the nAChR-Bound Dansyl-C_6-choline Fluorescence Spectrum. The binding of mAbs to the unblocked *A* or *B* ACh binding sites in the nAChR produced significant changes in the emission spectrum of bound dansyl-C_6-choline (Figure 3). The binding of both mAbs decreased the fluorescence emission from nAChR-bound dansyl-C_6-choline by ~60%. Although the binding of the *B1* mAb did not produce a chromatic shift in the emission maximum of

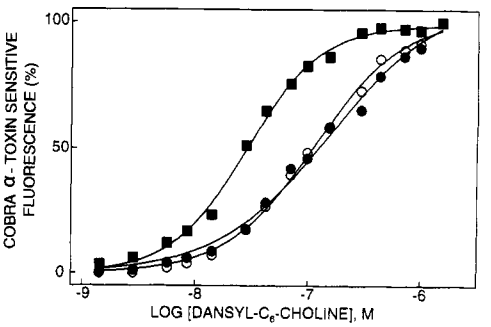

FIGURE 2: mAb effects on dansyl-C_6-choline binding to nAChR membranes. Incremental amounts of dansyl-C_6-choline were titrated into suspensions of nAChR (50 nM in suberyldicholine binding sites) that had been preincubated for 10 min with PCP (40 μM), ± an excess of cobra α-toxin (0.2 μM). The numerical difference between these two sets of data is plotted and represents the specific fluorescence associated with dansyl-C_6-choline binding. The excitation and emission wavelengths were 280 and 540 nm, respectively. The titration was performed in the absence of mAbs (■), in the presence of *A6* mAb (○), and in the presence of *B1* mAb (●). The average K_D ± SD values were 20 ± 14 (Valenzuela *et al.*, 1994), 117 ± 14, 75 ± 11 nM, respectively.

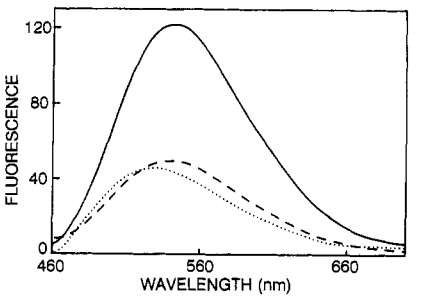

FIGURE 3: mAb effects on the emission spectrum of nAChR-bound dansyl-C_6-choline. Shown are the corrected emission spectra of dansyl-C_6-choline (0.4 μM) bound to the nAChR (0.4 μM in suberyldicholine binding sites) in the absence of mAbs (solid line) and in the presence of the *A6* (dotted line) or *B1* (dashed line) mAbs (0.4 μM). Emission spectra were measured with and without an excess of cobra α-toxin (4 μM), and the difference spectra are shown.

nAChR-bound dansyl-C_6-choline (Figure 3), the *A6* mAb blue shifted the bound dansyl-C_6-choline emission maximum from 540 to 529 nm. Because the FRET experiments described below typically required about 2 h to perform, the stability of the dansyl-C_6-choline–mAb–nAChR complexes was assessed by monitoring receptor-bound dansyl-C_6-choline emission for a period of 2 h. During this period the dansyl-C_6-choline emission was stable (data not shown).

mAb Effects on the Fluorescence Lifetime and Quantum Yield of Receptor-Bound Dansyl-C_6-choline. Because the FRET measurements also require a knowledge of the donor quantum yield, the effect of the mAbs on fluorescent lifetime of receptor-bound dansyl-C_6-choline was determined. Receptor-bound dansyl-C_6-choline displayed biexponential fluorescence decay (Table 1) with 5.7-ns (preexponential $a_1 = 0.64$) and 15.2-ns (preexponential $a_2 = 0.36$) fluorescence lifetimes, in agreement with our previously published values (Herz *et al.*, 1989). The binding of the *A6* mAb produced a significant change in both components of the dansyl-C_6-choline fluorescence lifetime to 4.9 (preexponential $a_1 = 0.75$) and 18.4 ns (preexponential $a_2 = 0.25$). Similarly, the binding of the *B1* mAb decreased the lifetimes to 4.5 (preexponential $a_1 = 0.69$) and 18.2 ns (preexponential $a_2 = 0.31$). The geometrically averaged lifetimes, therefore, decreased from 9.1 to 8.2 and 7.6 ns by the presence of *A6* and *B1*, respectively (Table 2). Using our previously determined values for the

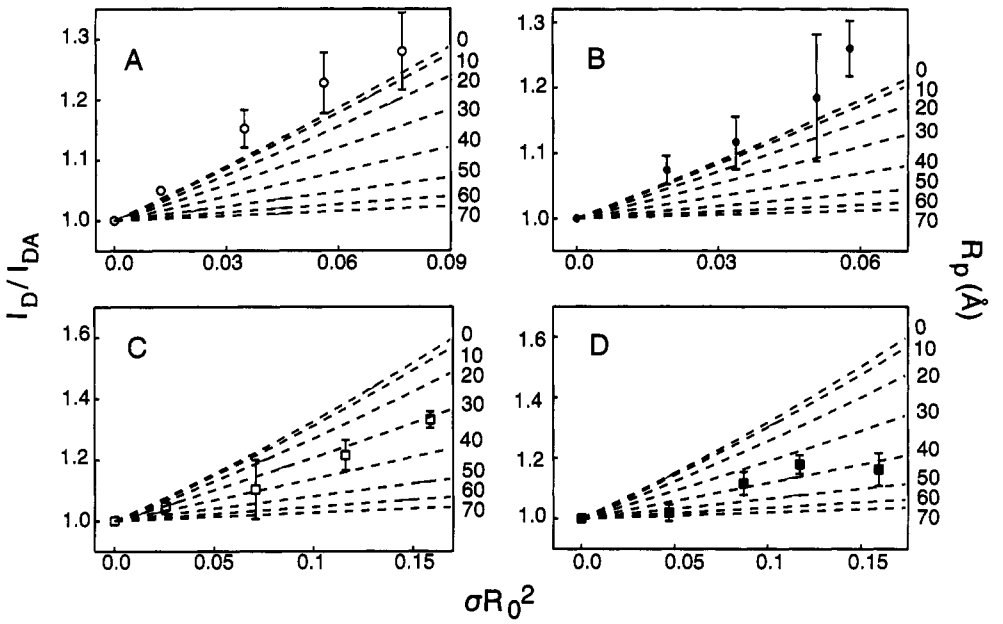

FIGURE 4: mAb effects on FRET between nAChR-bound dansyl-C_6-choline and the membrane acceptors. Plotted as points ± SD are the ratios of nAChR-bound dansyl-C_6-choline fluorescence (donor) in the absence (I_D) over the presence (I_{DA}) of the membrane-partitioned acceptor C_{18}-rhodamine (○, □) or C_{12}-eosin (●, ■), as a function of the surface density of acceptors (σ) times R_0^2. Panels A and B represent the FRET in the presence of *A6* mAb and panels C and D that in the presence of *B1* mAb. The excitation wavelength was 310 nm in all cases, whereas the emission wavelength was 540 and 500 nm for the experiments with C_{18}-rhodamine or C_{12}-eosin, respectively. For concentrations see legend to Figure 3.

Table 1: Effect of mAbs on the nAChR-Bound Dansyl-C_6-choline Fluorescence Lifetimes[a]

condition[b]	n^c	$a_1{}^d$	τ_1	$a_2{}^d$	τ_2	$\langle\tau\rangle^e$
no mAbs	11	0.64	5.7 ± 0.7	0.36	15.2 ± 1.0	9.1 ± 0.3
+*A6*	2	0.75	4.9 ± 0.8	0.25	18.4 ± 1.5	8.2 ± 0.1
+*B1*	2	0.69	4.5 ± 0.1	0.31	18.2 ± 0.9	7.6 ± 0.2

[a] Average ± SD. The measurements were made with nAChR (1.0 μM in suberyldicholine binding sites), dansyl-C_6-choline (1.0 μM), and PCP (500 μM) in buffer I. The excitation and emission wavelengths were selected with a Corning 7-54 filter and an Oriel 540-nm narrow-band interference filter. [b] mAbs (1.0 μM) were preincubated with nAChR for 90 min at 37 °C in plastic tubes. [c] Number of determinations. [d] Averaged normalized preexponential terms. [e] Geometrically averaged lifetimes.

Table 2: Parameters for FRET between Receptor-Bound Dansyl-C_6-choline and Membrane-Partitioned C_{18}-Rhodamine or C_{12}-Eosin ± mAbs

acceptor	condition	J^a ($\times 10^{13}$) (cm^6/mol)	$Q_D{}^b$	$R_0{}^c$ (Å)	$R_p{}^d$ (Å)
C_{18}-rhodamine	no mAbs	3.7[e]	0.22[e]	48[e]	39 ± 5[e]
	+ *A6*	3.5	0.20	47	≤0
	+ *B1*	3.7	0.19	47	31 ± 2
C_{12}-eosin	no mAbs	2.5[e]	0.22[e]	45[e]	31 ± 5[e]
	+ *A6*	2.6	0.20	44	≤0
	+ *B1*	2.4	0.19	44	40 ± 4

[a] Overlap integral defined under Experimental Procedures. [b] Donor quantum yield of receptor-bound dansyl C_6-choline as determined under Experimental Procedures. [c] Förster critical distance given under Experimental Procedures (assumptions: $\kappa^2 = {}^2/_3$ and $n = 1.4$). [d] Calculated transverse distance ± SD between the nAChR-bound dansyl-C_6-choline and the lipid membrane surface assuming the Off-Axis FRET model given under Experimental Procedures. [e] Value from Valenzuela *et al.* (1994).

fluorescence lifetime and quantum yield of dansyl-C_6-choline in buffer, 3.0 ns and 0.073, respectively (Herz *et al.*, 1989) and assuming the quantum yield to be proportional to the fluorescence lifetime (Berlman, 1971), the calculated quantum yields of receptor-bound dansyl-C_6-choline in the absence and presence of the *A6* and *B1* mAbs are 0.22, 0.20, and 0.19, respectively (Table 2).

Effect of the mAbs on the FRET Parameters. The energy-transfer parameters for the FRET between dansyl-C_6-choline and the membrane-partitioned acceptors were minimally affected by the binding of the *A6* and *B1* mAbs (Table 2). As described above, the mAbs decreased the dansyl-C_6-choline quantum yield by ~10%. The overlap integral for the dansyl-C_6-choline/C_{12}-eosin and dansyl-C_6-choline/C_{18}-rhodamine donor–acceptor pairs ranged between 3.5–3.7 × 10^{-13} and 2.4–2.6 × 10^{-13} cm^6/mol, respectively (Table 2). The R_0 values were 47–48 and 44–45 Å, respectively (Table 2). These FRET parameters are very similar to the previously determined values in the absence of mAbs (Table 2) (Valenzuela *et al.*, 1994).

mAb Effects on FRET between nAChR-Bound Dansyl-C_6-choline and the Membrane-Partitioned Acceptors. FRET between nAChR-bound dansyl-C_6-choline (donor) and the membrane probes (acceptors), C_{12}-eosin or C_{18}-rhodamine, was previously reported (Valenzuela *et al.*, 1994). Each of the membrane probes used is composed of a charged fluorophore attached to a hydrocarbon membrane anchor. With such a molecular configuration these probes would be expected to position themselves at the water–lipid interface and, thus, allow distance measurements between the ACh binding sites and the lipid membrane surface. Fluorescence quenching with 5-, 7-, 12-, and 16-doxylstearate or potassium iodide confirmed this nAChR membrane orientation for C_{18}-rhodamine (Arias *et al.*, 1993). In the absence of the mAbs the transverse distance between the ACh binding sites and the membrane surface was estimated to be ~35 Å (Valenzuela *et al.*, 1994).

Using this same approach, the effect of the *A6* and *B1* mAbs on the proximity of the mAb-free ACh binding site to the lipid membrane was examined. Figure 4 and Table 2 summarize the FRET measurements preformed with the *A6* and *B1* mAbs. The fluorescence of nAChR-bound dansyl-C_6-choline was calculated with eq 10. The ratios of the nAChR-bound dansyl-C_6-choline fluorescence in the absence

Table 3: mAb Effects on 5-Doxylstearate Quenching of nAchR-Bound Dansyl-C_6-choline and Membrane-Partitioned C_{18}-Rhodamine Fluorescence[a]

	C_{18}-rhodamine		dansyl-C_6-choline			
condition	K_Q[b] (M^{-1})	K_Q^{mAb}/K_Q^{0}[c]	K_Q[b] (M^{-1})	K_Q^{mAb}/K_Q^{0}[c]	corrected K_Q[d] (M^{-1})	corrected $K_Q^{w/o}/K_Q^{w/mAb}$[e]
no mAb	9.8 ± 0.2	1.0	0.06 ± 0.2	1.0	0.06 ± 0.2	1
+*A6* mAb	4.7 ± 0.3	0.48	1.3 ± 0.1	21.7	2.7 ± 0.2	45
+*B1* mAb	11.5 ± 0.6	1.2	0.5 ± 0.1	8.3	0.42 ± 0.1	7

[a] For experimental details see the legend of Figure 3. [b] Apparent steady-state Stern–Volmer quenching constants from least-squares fits to the plots in Figure 5. [c] The ratio of the observed quenching constants determined in the presence of one of the mAbs (K_Q^{mAb}) over the value determined in the absence of any mAb (K_Q^0). [d] The corrected quenching constant was calculated by dividing the observed dansyl-C_6-choline quenching constant by the appropriate K_Q^{mAb}/K_Q^0 ratio for 5-doxylstearate quenching of C_{18}-rhodamine fluorescence. [e] The ratio of the corrected constants for 5-doxylstearate quenching of dansyl-C_6-choline fluorescence in the absence over the presence of one of the mAbs.

of acceptors (I_D) divided by its fluorescence in the presence of acceptors (I_{DA}) were plotted as a function of acceptor surface density (σ) times R_0^2. The values for the acceptor surface density were determined in separate experiments for each nAChR–membrane preparation used in the presence of each mAb, as described by Valenzuela *et al.* (1992). Also shown in Figure 4 are theoretical plots (*dashed lines*) of I_D/I_{DA} vs σR_0^2 for various values of the transverse distance (R_P) between the specifically bound dansyl-C_6-choline and the lipid membrane surface that were generated by numerically solving eqs 2–9. The effect of the *A6* mAb was dramatically different from that of the *B1* mAb. In the presence of the *A6* mAb, the observed energy transfer (I_D/I_{DA}), with either C_{12}-eosin or C_{18}-rhodamine as acceptor, was greater than what would be predicted from the Off-Axis FRET model if the transverse distance between the *B* ACh binding site and the lipid membrane was less than zero (Figure 4A,B and Table 2). This suggests that the *A6* mAb induced the *B* ACh binding site to move in close proximity to the lipid membrane and that the Off-Axis FRET model used in the theoretical calculations in probably invalid when the *A6* mAb is present. In contrast, the presence of the *B1* mAb had little effect on FRET observed in the absence of the mAbs (Figure 4C,D and Table 2). The calculated distance between dansyl-C_6-choline bound to the *A* ACh binding site and the membrane surface ranged between 31 and 40 Å, which is essentially identical to the previously obtained distance in the absence of mAbs (31–39 Å) (Valenzuela *et al.*, 1994). This suggests that the *B1* mAb had little effect on the distance between the *A* ACh binding site and the lipid membrane.

mAb Effects on the Paramagnetic Quenching of nAChR-Bound Dansyl-C_6-choline. To confirm that the *A6* mAb induced an apparent movement of the high-affinity agonist binding site into close proximity to the lipid membrane, the relative ability of a short-range lipophilic quencher, 5-doxylstearate, to reduce the emission from specifically bound dansyl-C_6-choline was assessed. To control for the possibility that the mAbs might adsorb the 5-doxylstearate and thereby reduce the membrane partitioning of 5-doxylstearate, the ability of 5-doxylstearate to quench the fluorescence of a lipophilic fluorescent probe, C_{18}-rhodamine, which had been previously incorporated into the nAChR membranes, was also examined.

Figure 5 and Table 3 summarize the results of these quenching experiments. In the absence of the mAbs, 5-doxylstearate quenched membrane–partitioned C_{18}-rhodamine fluorescence 160-fold more effectively than specifically bound dansyl-C_6-choline fluorescence. This is consistent with the observation that in the absence of mAbs the dansyl-C_6-choline binding site is a distance from the lipid membrane (Valenzuela *et al.*, 1994). The addition of the *A6* mAb was associated with about a 50% reduction of the ability of 5-doxylstearate

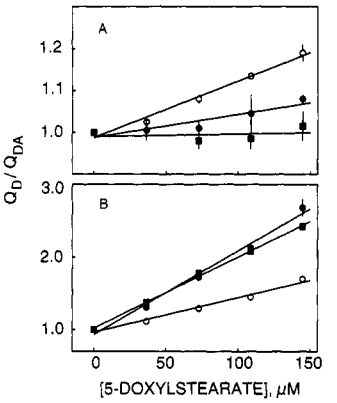

FIGURE 5: mAb effects on paramagnetic quenching of nAChR-bound dansyl-C_6-choline and membrane-partitioned C_{18}-rhodamine by 5-doxylstearate. Plotted as points ± SD are the ratios of nAChR-bound dansyl-C_6-choline (panel A) or C_{18}-rhodamine (panel B) fluorescence, in the absence (I_D) divided by their fluorescence in the presence (I_{DA}) of increasing concentrations of 5-doxylstearate. The quenching was measured in the absence of any mAbs (■), in the presence of *A6* mAb (○), or in the presence of *B1* mAb (●). The excitation and emission wavelengths were 310 and 540 nm for panel A and 550 and 600 nm for panel B, respectively. For concentrations see legend to Figure 4.

to quench C_{18}-rhodamine fluorescence, suggesting that the *A6* mAb preparation reduced the membrane concentration of the 5-doxylstearate by adsorbing about 50% of the 5-doxylstearate. In contrast, the *B1* mAb had little or no effect on the 5-doxylstearate partitioning. Because the mAbs differentially affected the membrane partitioning of 5-doxylstearate, it was necessary to correct the apparent dansyl-C_6-choline quenching constants. This was accomplished by dividing the observed dansyl-C_6-choline Stern–Volmer quenching constants (K_Q) by the ratios of the C_{18}-rhodamine Stern–Volmer quenching constants in the absence over the presence of mAb. After the differential 5-doxylstearate partitioning was corrected for, the addition of the *A6* mAb was associated with about a 45-fold increase in the dansyl-C_6-choline quenching constant and therefore increased accessibility of 5-doxylstearate to receptor-bound dansyl-C_6-choline. Importantly, in the presence of the *A6* mAb, the magnitude of the C_{18}-rhodamine quenching constant was within a factor of 2 of the corrected dansyl-C_6-choline quenching constant, indicating that despite the greater size of the dansyl-C_6-choline–nAChR complex relative to C_{18}-rhodamine, 5-doxylstearate is highly accessible to the receptor-bound dansyl-C_6-choline and confirms that the *A6* mAb induced the low-affinity ACh binding site to move into close proximity to the lipid membrane. The addition of the *B1* mAb, on the other hand, was associated with a 7-fold increase in the dansyl-C_6-choline quenching constant. Because the C_{18}-rhodamine quenching constant is

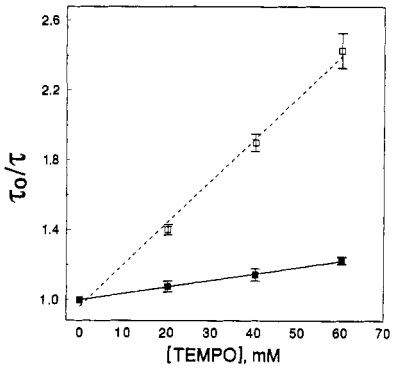

FIGURE 6: Stern–Volmer plots of the effect of Tempo on the fluorescence lifetime of dansyl-C_6-choline and C_{18}-rhodamine in 1-butanol. Dansyl-C_6-choline (□) and C_{18}-rhodamine (■) were dissolved in 1-butanol at 3 μM final concentration and titrated with 4.75 M Tempo (dissolved in 1-butanol). Dansyl-C_6-choline samples were excited at about 340 nm with a Corning 7-60 interference filter in the path of the excitation beam, and the emission was monitored through a Corning 3-71 cutoff filter. The C_{18}-rhodamine samples were excited at 560 nm by using an Oriel 560-nm interference filter, and the emission was monitored through a Corning 3-66 cutoff filter.

Table 4: Relative Sensitivity of Dansyl-C_6-choline and C_{18}-Rhodamine to Quenching by Tempo in 1-Butanol

fluorophore	K_Q'[a] (M^{-1})	$\langle\tau\rangle$[b] (ns)	k_q[c] × 10^{-9} (M^{-1} s^{-1})	ratio of k_qs dansyl-C_6-choline/ C_{18}-rhodamine
dansyl-C_6-choline	24.9	14.5	1.7	1.2
C_{18}-rhodamine	3.7	2.6	1.4	

[a] K_Q', average (three determinations) Stern–Volmer quenching constant derived from the analysis of the lifetime data of Figure 6. [b] τ, average fluorescence lifetime (at least four determinations). [c] k_q, average bimolecular quenching constant using eq 11.

still 27-fold greater than the dansyl-C_6-choline quenching constant, 5-doxylstearate has a limited accessibility to the receptor-bound dansyl-C_6-choline and, which thus confirms that the *B1* mAb did not induce the high-affinity ACh binding site to move in close proximity to the lipid membrane.

Relative Sensitivity of Dansyl-C_6-choline and C_{18}-Rhodamine to Paramagnetic Quenching. Because fluorophores can potentially differ in their intrinsic sensitivities to paramagnetic quenchers, the relative sensitivity of dansyl-C_6-choline and C_{18}-rhodamine fluorescence to quenching by Tempo in 1-butanol was assessed. To evaluate the relative quenching independent of nondiffusional factors, quenching was measured as a reduction of fluorescence lifetime. Stern–Volmer plots of these results are shown in Figure 6. Table 4 presents the slopes, K_Q', of these plots and the calculated bimolecular quenching rate constants, k_q. When correction for the fluorescence lifetime is made, Tempo is about equally able to quench either dansyl-C_6-choline or C_{18}-rhodamine fluorescence. This indicates that the differences in paramagnetic quenching of receptor-bound dansyl-C_6-choline and membrane-partitioned C_{18}-rhodamine fluorescence are not due to an intrinsic difference in the sensitivity of these fluorophores to paramagnetic quenching.

DISCUSSION

The high- (*A*) and low- (*B*) affinity ACh binding sites on the nAChR are localized about 50–70 Å away from each other (Zingsheim *et al.*, 1982; Johnson *et al.*, 1984) at or near the α–γ and α–δ subunit interfaces, respectively (Pedersen & Cohen, 1990; Sine & Claudio, 1991). In this paper, the effects of two mAbs, which block ligand binding to either the high- (*A6* mAb) or low- (*B1* mAb) affinity ACh binding sites, on the structure of the nAChR were examined. These mAbs produced significant and distinct conformational changes in the nAChR. Both mAbs decreased somewhat the affinity and fluorescence lifetime of nAChR-bound dansyl-C_6-choline, indicating that both mAbs induced conformational changes that affected the mAb-free ACh binding site. The effects of *A6* or *B1* mAbs on the conformation of the nAChR differed dramatically from one another in terms of their ability to alter the distance of closest approach between the mAb-free ACh binding site and the membrane surface. FRET measurements indicated that the binding of *A6* to the *A* ACh binding site induced a major conformational change in the nAChR, where the unblocked *B* ACh binding site moved ~35 Å closer to the lipid membrane surface.

Paramagnetic fluorescence quenching experiments confirmed that the low-affinity ACh site at the α–δ subunit interface moved in close proximity to the lipid membrane domain because a short-range lipophilic quencher, 5-doxylstearate, became 45-fold more accessible to receptor-bound dansyl-C_6-choline. The magnitude of the 5-doxylstearate accessibility to receptor-bound dansyl-C_6-choline was within a factor of 2 of its accessibility to the membrane-partitioned probe, C_{18}-rhodamine. The differences in 5-doxylstearate accessibility to membrane partitioned C_{18}-rhodamine and receptor-bound dansyl-C_6-choline were not due to intrinsic differences in their sensitivity to paramagnetic quenching, because the bimolecular quenching constants for Tempo quenching of dansyl-C_6-choline and C_{18}-rhodamine fluorescence in 1-butanol were essentially identical (Figure 6 and Table 4).

On the basis of 5-doxylstearate quenching, the *B1* mAb appeared to induce a much smaller increase (7-fold) in the accessibility of the *A* ACh binding site to the liopophilic quenchers than the *A6* mAb (Figure 5; Table 3). However, the magnitude of the 5-doxylstearate accessibility to receptor-bound dansyl-C_6-choline in the presence of the *B1* mAb was still 27-fold greater than its accessibility to membrane-partitioned C_{18}-rhodamine. Moreover, the dansyl-C_6-choline FRET measurements indicated no significant *B1* mAb-induced change in the distance from the *A* site to the membrane surface. Consequently, despite an increase in the apparent accessibility of a lipophilic quencher to the *A* ACh binding site, the *B1* mAb did not appreciably move the *A* site into close proximity to the membrane surface.

An alternative interpretation of these results might be that the *A* and *B* ACh binding sites are intrinsically not equidistant from the lipid membrane surface. The effect of the mAbs in selectively blocking dansyl-C_6-choline binding was simply to reveal that the *A* ACh site is 31–40 Å and the *B* ACh site is ~0 Å from the membrane surface. The difficulty with this interpretation is that if the *A* ACh site was 31–40 Å and the *B* ACh site was ~0 Å from the membrane surface in the absence of mAbs, then the average transverse distance between the ACh sites and the membrane surface would be substantially less than the observed 31–39 Å. Therefore, this alternative interpretation is unlikely but justifies additional experimental study.

Although the results indicate that the *A6* mAb alters the proximity of the *B* ACh binding site to the lipid membrane surface, the extent of the *A6* mAb-induced structural perturbations of the nAChR is, however, unclear. The *A6* mAb-induced reduction in the distance between the ACh binding site and membrane surface could have occurred as a result of either a full or partial movement of the nAChR. As

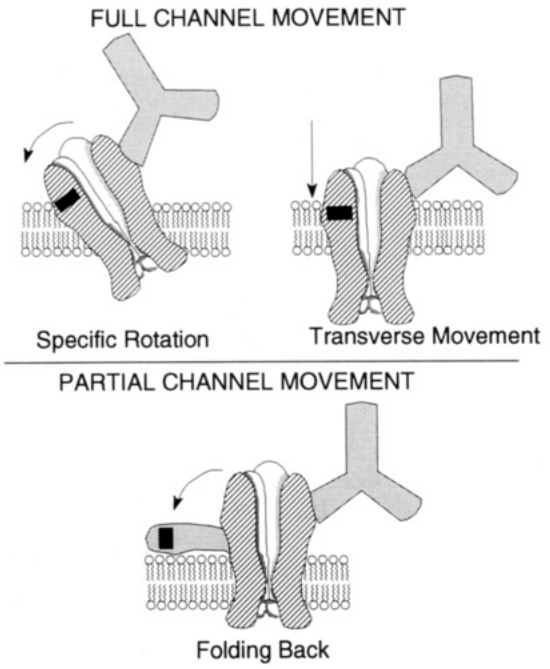

FIGURE 7: Schematic representation of the possible effects of the *A6* mAbs on the nAChR. The upper panel depicts two types of possible full movements of the nAChR that would result in the movement of the low-affinity ACh binding site to be in close proximity to the lipid membrane: (1) a specific rotation of the receptor about its major symmetry axis that would make it appear tilted and (2) a transverse movement of the nAChR such that it appears to have been pushed into the lipid membrane. The lower panel depicts a possible partial movement of the nAChR induced by the *A6* mAb. For the partial movement of the receptor only a portion of the receptor, which includes the low-affinity ACh binding site, folds back like a flower petal into the lipid membrane. The filled rectangles represent the low-affinity ACh binding site. The representation of the nAChR is from Unwin (1993).

illustrated in Figure 7, a full movement of the receptor would involve either a specific rotation of its major symmetry axis or a transverse movement of its extracellular domain into the lipid membrane; a partial movement would involve a folding or peeling back, like a flower petal, of a portion of the receptor into the lipid membrane. Because a full nAChR movement would involve a shifting of the extracellular and perhaps cytoplasmic domains into the lipid membrane and the exposure of transmembrane domains to extracellular and cytoplasmic space, very large areas of normally hydrophilic surfaces would have to be converted into hydrophobic surfaces and, similarly, normally hydrophobic surfaces would have to be converted into hydrophilic surfaces. Viewed thermodynamically, a full movement would appear to be energetically more expensive than a partial movement, and therefore, the more plausible physical interpretation of the results is that the *A6* mAb induced a partial movement of the receptor. However, there currently is little evidence in the literature for the existence of large movements in the receptor. Clearly, other biophysical approaches must be utilized to delineate the scope of the mAb-induced conformational changes reported here.

It is worth noting that the conformational changes described in this paper were induced by bivalent mAbs. Fab fragments of these mAbs were successfully generated but displayed ~50-fold lower affinity than the native mAbs (data not shown). The very large amounts of Fab fragments that would be necessary to perform the fluorescence measurements are extremely difficult to obtain, produce substantial turbidity, and interfere with the membrane partitioning of the lipophilic probes.

Whether these mAb-induced conformational states even partially resemble a physiologic conformation of the nAChR is unclear. The results suggest significant flexibility of at least the portion of the nAChR that forms the low-affinity ACh binding site and, therefore, show that mAbs can induce major conformational changes in the nAChR. mAb-induced changes in the surface exposure of plasma membrane proteins could have implications both in autoimmune diseases and in the use of mAbs for molecular structural studies of the nAChR. For autoimmune diseases, a mAb-induced change in surface exposure could lead to the exposure of a neoepitope toward which additional immune responses could be directed, further aggravating the disease. For mAbs use in molecular structural studies, mAbs-induced changes in the extracellular, membrane, or cytoplasmic exposure of the receptor could yield conflicting information on the location of different nAChR domains, as the binding of mAbs might differentially uncover side chains to labeling reagents. Additionally, mAbs may dramatically shift the position of the epitope prior to electron microscopic image analyses to reveal a false position of the epitope.

A major direction of current research on the nAChR is toward understanding the molecular basis of acetylcholine activation of the channel. From this perspective, the present results, also, suggest a direction for future research, namely, an exploration of time-dependent changes in the distance of closest approach between the ACh binding sites and the lipid membrane. The apparent flexibility of one of the ACh binding sites may be an element in the channel opening/closing mechanism that could be examined by measuring FRET between the ACh binding sites and the lipid membrane in a stop-flow apparatus.

In conclusion, the *A6* and *B1* anti-nAChR mAbs produced significant, but different, global conformational changes in the receptor. Both mAbs induced a conformational change that appeared to involve rearrangements in at least the extracellular domain of the receptor. However, the *A6* mAb, but probably not the *B1* mAb, induced a dramatic shift in the distance of closest approach between the low-affinity ACh binding site at the α–δ subunit interface and the lipid membrane. A possible interpretation of these results would be that the portion of the receptor associated with the low-affinity ACh binding site is highly flexible and capable of moving into close proximity to the lipid membrane.

ACKNOWLEDGMENT

This work is from the dissertation submitted by C.F.V. in partial fulfillment of the requirements for the Ph.D. degree in biomedical sciences at the University of California, Riverside. We are grateful to Anthony Nguyen and Rebecca Wilson for assistance with the preparation of the nAChR-rich membranes. We thank Drs. Carl Ware and Kenneth Dorshkind for helpful comments and technical assistance.

REFERENCES

Arias, H. R., Valenzuela, C. F., & Johnson, D. A. (1993) *J. Biol. Chem. 268*, 6348–6355.

Arnand, R., Conroy, W. G., Schoepfer, R., Whiting, P., & Lindstrom, J. (1991) *J. Biol. Chem. 266*, 11192–11198.

Berlman, I. B. (1971) *Handbook of Fluorescence Spectra of Aromatic Compounds*, p 15, Academic Press, New York.

Chen, R. F. (1965) *Science 150*, 1593–1595.

Chinchetru, M. A., Marquez, J., Garciá-Borrón, J. C., Richman, D. P., & Martínez-Carrión, M. (1989) *Biochemistry 28*, 4222–4229.

Conti-Tronconi, B. M., Tang, F., Diethelm, B. M., Spencer, S. R., Reinhardt-Maelicke, S., & Maelicke, A. (1990) *Biochemistry 29*, 6221–6230.
Dowding, A. J., & Hall, Z. W. (1987) *Biochemistry 26*, 6372–6381.
Fels, G., Plumer-Wilk, R., Schreiber, M., & Maelicke, A. (1986) *J. Biol. Chem. 261*, 15746–15754.
Galzi, J. L., Revah, F., Bessis, A., & Changeux, J.-P. (1991) *Annu. Rev. Pharmacol. 31*, 37–72.
Heidmann, T., Oswald, R. E., & Changeux, J.-P. (1983) *Biochemistry 22*, 3112–3127.
Herz, J. M., Johnson, D. A., & Taylor, P. (1989) *J. Biol. Chem. 264*, 12439–12448.
Johnson, D. A., & Yguerabide, J. (1985) *Biophys. J. 48*, 949–955.
Johnson, D. A., Voet, J., & Taylor, P. (1984) *J. Biol. Chem. 259*, 5717–5725.
Karlin, A. (1991) *Harvey Lect. 85*, 71–107.
Karlin, A. (1993) *Curr. Opin. Neurobiol. 3*, 299–309.
Karlin, B., Lawrence, J., Linstrom, J., & Merlie, J. (1986) *Proc. Natl. Acad. Sci. U.S.A. 83*, 498–502.
Karlsson, E., Arnberg, H., & Eaber, P. (1971) *Eur. J. Biochem. 21*, 1–16.
Klymkowsky, M. W., & Stroud, R. M. (1979) *J. Mol. Biol. 128*, 319–334.
Lei, S., Raftery, M. A., & Conti-Tronconi, B. M. (1993) *Biochemistry 32*, 91–100.
Lindstrom, J. (1986) *Trends Neurosci. 9*, 401–407.
London, E. (1982) *Mol. Cell. Biochem. 45*, 181–188.
Maelicke, A., Fels, G., Plumer-Wilk, R., & Schreiber, M. (1988) *J. Recept. Res. 8*, 133–142.
Neubig, R. R., & Cohen, J. B. (1979) *Biochemistry 18*, 5464–5475.
Pedersen, S. E., & Cohen, J. B. (1990) *Proc. Natl. Acad. Sci. U.S.A. 87*, 2785–2789.
Role, L. W. (1992) *Curr. Opin. Neurobiol. 2*, 254–262.
Sine, S. M., & Claudio, T. (1991) *J. Biol. Chem. 266*, 19369–19377.
Tzartos, S. J., Chung, M. T., Demange, P., Loutrari, H., Mamalaki, A., Marraud, M., Papadoulli, I., Sakarellos, C., & Tsikaris, V. (1991) *Mol. Neurobiol. 5*, 1–29.
Unwin, N. (1993) *J. Mol. Biol. 229*, 1101–1124.
Valenzuela, C. F., Kerr, J. A., & Johnson, D. A. (1992) *J. Biol. Chem. 267*, 8238–8244.
Valenzuela, C. F., Weign, P., Yguerabide, J., & Johnson, D. A. (1994) *Biophys. J. 66*, 674–682.
Ware, C. F., Donato, N. J., & Dorshkind, K. (1985) *J. Immunol. Methods 85*, 353–361.
Yguerabide, J. (1972) *Methods Enzymol. 26*, 498–578.
Yguerabide, J. (1994) *Biophys. J. 66*, 683–693.
Zingsheim, H. P., Barrantes, F. J., Frank, J., Haniche, W., & Neugebauer, D.-C. (1982) *Nature 299*, 81–84.